J. Fluid Mech. (1989), *vol.* 208, *pp.* 609–637
Printed in Great Britain

Inviscid spatial stability of a compressible mixing layer

By T. L. JACKSON[1] AND C. E. GROSCH[2]

[1] Department of Mathematics and Statistics, Old Dominion University, Norfolk, VA 23529, USA

[2] Department of Oceanography and Department of Computer Science, Old Dominion University, Norfolk, VA 23529, USA

(Received 26 May 1988 and in revised form 14 February 1989)

We present the results of the inviscid spatial stability of a parallel compressible mixing layer. The parameters of this study are the Mach number of the moving stream, the ratio of the temperature of the stationary stream to that of the moving stream, the frequency, and the direction of propagation of the disturbance wave. Stability characteristics of the flow as a function of these parameters are given. It is shown that if the Mach number exceeds a critical value there are always two groups of unstable waves. One of these groups is fast with phase speeds greater than $\frac{1}{2}$ and is supersonic with respect to the stationary stream. The other is slow with phase speeds less than $\frac{1}{2}$ and supersonic with respect to the moving stream. Phase speeds for the neutral and unstable modes are given, as well as growth rates for the unstable modes. Finally, we show that three-dimensional modes have the same general behaviour as the two-dimensional modes but with higher growth rates over some range of propagation direction.

1. Introduction

An understanding of the stability characteristics of compressible mixing layers is of fundamental interest and is also extremely important in view of the projected use of the scramjet engine for the propulsion of hypersonic aircraft. Knowledge of these characteristics may allow one, in principle, to control the downstream evolution of such flows. This is particularly important because of the observed increase in the flow stability at high Mach numbers (Brown & Roshko 1974; Chinzei *et al.* 1986; and Papamoschou & Roshko 1986, 1988). Because of the gain in stability, natural transition may occur at downstream distances which are larger than practical combustor lengths. A number of techniques to enhance mixing are discussed by Kumar, Bushnell & Hussaini (1987). A detailed understanding of the linear stability characteristics of compressible mixing layers will be of aid in mixing enhancement.

In this paper we will examine the inviscid stability of a compressible mixing layer, the interfacial region between a moving gas at $+\infty$ and a stationary gas at $-\infty$. The stability of the mixing layer in a compressible fluid has not been studied as extensively as the same flow in an incompressible fluid. The basic formulation of the theory for the stability of compressible shear flows, both free and wall bounded, is due to Lees & Lin (1946), and Dunn & Lin (1955) first showed the importance of three-dimensional disturbances for the stability of these flows.

There have been a number of theoretical studies of the stability of compressible

free-shear layers in recent years. These include that of Tam & Hu (1988) who examined the stability of the compressible mixing layer in a channel using the hyperbolic tangent profile, and Zhuang, Kubota & Dimotakis (1988) who also studied the mixing layer with the hyperbolic tangent profile and found decreasing amplification with increasing Mach number. Ragab (1988) carried out a numerical solution of the two-dimensional compressible Navier–Stokes equations for the wake/mixing layer behind a splitter plate, and then carried out a linear stability analysis of the computed mean flow. He found that increasing the Mach number leads to a strong stabilization of the flow and that the disturbances have large dispersion near the splitter plate and smaller dispersion downstream. Ragab & Wu (1988) examined the viscous and inviscid stability of a compressible mixing layer using both the hyperbolic tangent and Sutherland profiles. They found that if the Reynolds number was greater than 1000, the disturbances could be calculated very accurately from inviscid theory. In addition, they reported that non-parallel effects are negligible. It seems that in this study their main interest was in determining the dependence of the maximum growth rate of the disturbances on the velocity ratio of the mixing layer. They concluded that the maximum growth rate depends on the velocity ratio in a complex way, with the maximum growth rate appearing at a particular non-zero velocity ratio.

Earlier studies of the stability of compressible mixing layers include those of Lessen, Fox & Zien (1965, 1966) and Gropengiesser (1969). The inviscid temporal stability of the compressible mixing layer to two- and three-dimensional disturbances was studied by Lessen *et al.* for subsonic disturbances (1965) and supersonic disturbances (1966). They assumed that the flow was isoenergetic and, as a consequence, the temperature of the stationary gas was always greater than that of the moving gas. In fact, because the ratio of the temperature at $\pm\infty$ varies as the square of the Mach number, the stationary gas is much hotter than the moving gas at even moderately supersonic speeds. Gropengiesser (1969) re-examined this problem, but without using the isoenergetic assumption. Consequently, he was able to treat the ratio of the temperatures of the stationary and moving gas as a parameter. He carried out inviscid spatial stability calculations for the compressible mixing layer using a generalized hyperbolic tangent profile (see his equation (2.27)) to approximate the Lock profile for temperature ratios of 0.6, 1.0 and 2.0 and for Mach numbers between 0 and 3. We will discuss Gropengiesser's results in comparison with ours in a later section.

Gill (1965) found that 'top hat' jets and wakes have an infinite set of unstable modes. These arise from multiple reflection of sound waves within the layer formed by the discontinuity at the edges of the jets and wakes. Blumen, Drazin & Billings (1975) and Drazin & Davey (1977) investigated the temporal stability of a compressible mixing layer. They used a hyperbolic tangent profile for the velocity and assumed that the temperature was a constant throughout the layer. In both of these studies multiple instability modes were found near a Mach number of one. Quite recently, multiple modes were also found in a temporal stability analysis of the compressible mixing layer without invoking the assumptions of a hyperbolic tangent velocity profile and that of a constant temperature throughout the layer (Macaraeg, Streett & Hussaini 1988). Mack (1984) carried out an extensive study of the inviscid spatial eigenfunctions of the compressible boundary layer. He found that there was an infinite set of discrete modes of which the first was a vortical mode and all the others were acoustic modes. These acoustic modes can be visualized as sound waves

undergoing reflection between the wall and the sonic line. The first of the acoustic modes is the most unstable of the inviscid compressible boundary-layer modes and the maximum growth rate is for its two-dimensional form.

The results reported here were obtained as the first part of a study of the stability of compressible mixing layers in which a diffusion flame is embedded (Jackson & Hussaini 1988). We are primarily interested in solving the stability problem over a large Mach-number range. As will be seen below, it appears necessary to only consider the range $0 \leqslant M \leqslant 10$ in order to be able to deduce the asymptotic ($M \rightarrow \infty$) behaviour of the solutions. In order to understand the effect of the heat release on the stability of this flow, one must first understand the stability characteristics of a non-reacting flow. It is well known (see Mack 1987 for a review) that the inviscid theory is a reliable guide for understanding the stability of compressible shear flows at moderate and larger Reynolds numbers. Thus we consider only the inviscid spatial stability problem.

We begin this study by taking the mean velocity profile in the mixing layer to be that of the Lock profile (Lock 1951). In the course of carrying out the stability calculations for this profile with different sets of values of the basic parameters, we noted some quite interesting features of the solutions, particularly at higher Mach numbers. In order to examine these features in more detail, we replaced the Lock profile with a hyperbolic tangent profile. This is a reasonable approximation to the Lock profile at low and moderate Mach numbers and has been used by many investigators in studying the stability of incompressible mixing layers, see Michalke (1972), Monkewitz & Huerre (1982), and Ho & Huerre (1984), as well as compressible mixing layers. More importantly from our point of view, we can obtain certain results analytically if we use the hyperbolic tangent profile to approximate the velocity distribution in the mixing layer. Our aim is to classify the neutral and unstable solutions, over a wide range of Mach numbers, using this model. Results for the Lock & Sutherland profiles will be presented in a future paper, and will be compared with these results. We expect quantitative differences, especially at higher Mach numbers.

In §2 we given the basic equations governing the mean flow and the small-amplitude disturbance equation. The boundary condition and the numerical method are also discussed in this section. Section 3 contains a presentation of our results and conclusions are given in §4.

2. Formulation of the problem

We consider the stability of a compressible mixing layer, with zero pressure gradient, which separates two streams of different speeds and temperatures. We assume that the mean flow is governed by the compressible boundary-layer equations (Stewartson 1964). The x-axis is taken along the direction of the flow, the y-axis normal to the flow, and the z-axis in the cross-stream direction. We let (U, V, 0) be the velocity and T the temperature of this mean flow. All of the variables are non-dimensionalized using the free-stream values at $y = +\infty$. In what follows we assume that the Prandtl number is unity.

The mean flow equations are first transformed into the incompressible form by means of the Howarth–Dorodnitzyn transformation

$$Y = \int_0^y \rho \, \mathrm{d}y, \quad \hat{V} = \rho V + U \int_0^y \rho_x \, \mathrm{d}y, \tag{2.1}$$

where ρ is the density and, because the pressure gradient is zero,

$$\rho T = 1. \tag{2.2}$$

Next we transform to the similarity variable

$$\eta = \frac{Y}{2(xC)^{\frac{1}{2}}}, \tag{2.3}$$

where C is the constant in Chapman's (1950) linear viscosity law

$$\mu = CT. \tag{2.4}$$

These equations have as a solution the similarity solution given by Lock (1951). However, as discussed in the introduction, we assume here that

$$U = \tfrac{1}{2}(1+\tanh(\eta)), \tag{2.5}$$

which approximates the Lock profile and can be handled analytically. This profile also satisfies the boundary conditions

$$U \to 1 \quad \text{as} \quad y \to +\infty, \qquad U \to 0 \quad \text{as} \quad y \to -\infty. \tag{2.6}$$

As is well known, the temperature distribution can be expressed in terms of the velocity field. The temperature boundary conditions are

$$T \to 1 \quad \text{as} \quad y \to +\infty, \qquad T \to \beta_T \quad \text{as} \quad y \to -\infty. \tag{2.7}$$

This yields

$$T = 1-(1-\beta_T)(1-U)+\tfrac{1}{2}(\gamma-1)M^2U(1-U), \tag{2.8}$$

where γ is the ratio of specific heats and M is the Mach number at $+\infty$. If β_T is less than one, the stationary gas is relatively cold compared to the moving stream, and if β_T is greater than one it is relatively hot.

The flow field is perturbed by introducing wave disturbances in the velocity, pressure, temperature and density with amplitudes which are functions of η. For example, the pressure perturbation is

$$p = \Pi(\eta)\exp[\mathrm{i}(\alpha x+\beta z-\omega t)], \tag{2.9}$$

with Π the amplitude, α and β the wavenumbers in the downstream (x) and cross-stream (z) directions, respectively, and ω the frequency which is taken to be real. As mentioned in the introduction, we are only treating the spatial stability problem. Substituting (2.9) for the pressure perturbation and similar expressions for the other flow quantities into the inviscid compressible equations yields the ordinary differential equations for the perturbation amplitudes (Lees & Lin 1946; Dunn & Lin 1955). It is straightforward to derive a single equation governing Π, given by

$$\Pi''-\frac{2U'}{U-c}\Pi'-T[(\alpha^2+\beta^2)T-\alpha^2M^2(U-c)^2]\Pi = 0. \tag{2.10}$$

Here, c is the complex wave velocity

$$c = \frac{\omega}{\alpha}, \tag{2.11}$$

and primes indicate differentiation with respect to the similarity variable η.

It is convenient to transform (2.10) to a form analogous to that for two-dimensional disturbances. To this end let

$$\hat{\alpha}^2 = \alpha^2+\beta^2. \tag{2.12}$$

Thus, $$\alpha = \hat{\alpha}\cos(\theta), \quad \beta = \hat{\alpha}\sin(\theta), \tag{2.13}$$

with θ the angle of propagation of the disturbance wave with respect to the flow direction. Further, define $\hat{M}$ and $\hat{\Pi}$ by

$$\hat{\alpha}\hat{M} = \alpha M, \quad \hat{\alpha}\hat{\Pi} = \alpha \Pi. \tag{2.14}$$

Applying this transformation to (2.10) yields

$$\hat{\Pi}'' - \frac{2U'}{U-c}\hat{\Pi}' - \hat{\alpha}^2 T[T - \hat{M}^2(U-c)^2]\hat{\Pi} = 0. \tag{2.15}$$

From the transformation we have

$$\hat{M} = M\cos(\theta), \tag{2.16}$$

$$c = \frac{\omega}{\alpha} = \frac{\omega}{\hat{\alpha}\cos(\theta)}. \tag{2.17}$$

Here $\hat{\alpha}$ is complex. The real part of $\hat{\alpha}$ is the magnitude of the wavenumber, while the imaginary part of $\hat{\alpha}$ indicates whether the disturbance is amplified, neutral, or damped depending on whether $\hat{\alpha}_i$ is negative, zero, or positive assuming positive group velocity. The phase speed, c_{ph}, is given by $\omega/\hat{\alpha}_r$. For a neutral wave the phase speed will be denoted by c_N. Finally, note that T is only a function of M and U, and does not change with the angle of propagation.

The boundary conditions for $\hat{\Pi}$ are obtained by considering the limiting form of (2.15) as $\eta \to \pm\infty$. The solutions to (2.15) are of the form

$$\hat{\Pi} \to \exp(\pm \Omega_\pm \eta), \tag{2.18}$$

where $$\Omega_+^2 = \hat{\alpha}^2[1 - \hat{M}^2(1-c)^2], \quad \Omega_-^2 = \hat{\alpha}^2\beta_T[\beta_T - \hat{M}^2c^2]. \tag{2.19}$$

Let us define $c_\pm$ to be the values of the phase speed for which $\Omega_\pm^2$ vanishes. Thus,

$$c_+ = 1 - \frac{1}{\hat{M}}, \quad c_- = \frac{\beta_T^{\frac{1}{2}}}{\hat{M}}. \tag{2.20}$$

Note that c_+ is the phase speed of a sonic disturbance in the moving stream and c_- is the phase speed of a sonic disturbance in the stationary stream. At

$$M = M_* \equiv \frac{1 + \beta_T^{\frac{1}{2}}}{\cos(\theta)} \tag{2.21}$$

$c_\pm$ are equal.

The nature of the disturbances and the appropriate boundary conditions can now be illustrated by reference to figure 1, where we plot $c_\pm$ versus $\hat{M}$ for a typical value of β_T. In what follows we assume that $\hat{\alpha}_r^2 > \hat{\alpha}_i^2$. These curves divide the $(c_r, \hat{M})$-plane into four regions, where c_r is the real part of c. If a disturbance exists with an $\hat{M}$ and c_r in region 1, then Ω_+^2 and Ω_-^2 are both positive, and the disturbance is subsonic at both boundaries. In region 3, both Ω_+^2 and Ω_-^2 are negative and hence the disturbance is supersonic at both boundaries. In region 2, Ω_+^2 is positive and Ω_-^2 is negative, and the disturbance is subsonic at $+\infty$ and supersonic at $-\infty$, and we classify it as a fast mode. Finally, in region 4, Ω_+^2 is negative and Ω_-^2 is positive so the disturbance is supersonic at $+\infty$ and subsonic at $-\infty$, and we classify it as a slow mode.

If the disturbance wave is subsonic at both $\pm\infty$ (region 1), one can choose the appropriate sign for $\Omega_\pm$ and have decaying solutions. We therefore have an eigenvalue problem. If the disturbance is supersonic at either, or both, boundaries

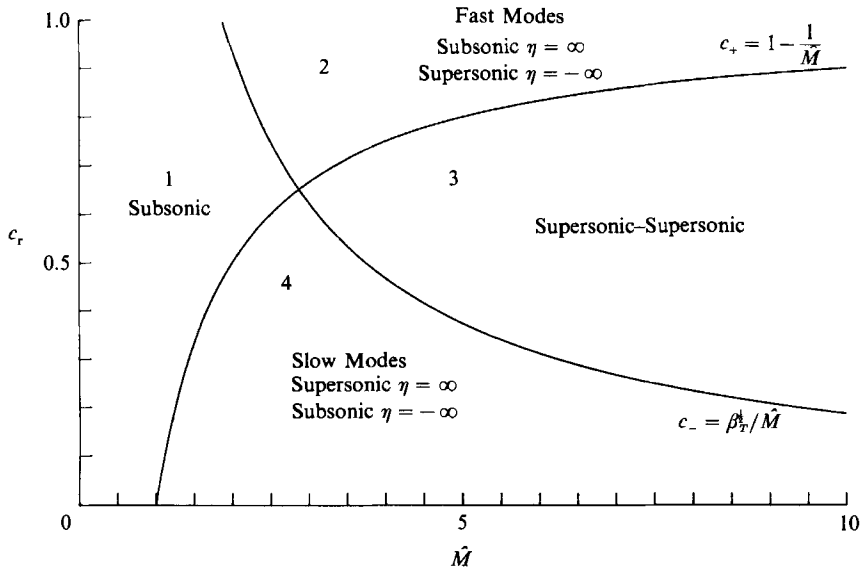

FIGURE 1. Plots of the sonic speeds $c_\pm$ versus Mach number for $\beta_T = 3.5$.

then the asymptotic solutions are purely oscillatory. These solutions are of two types. It is clear that the oscillatory solutions are either incoming or outgoing waves. If one assumes that only outgoing waves are permitted, the problem of finding solutions in regions 2, 3, or 4 is again an eigenvalue problem wherein one chooses, as boundary condition, the solutions to (2.15) which yields outgoing waves in the far field.

However if one permits both incoming and outgoing waves in the far field it is obvious that there are always solutions for any c in regions 2, 3, and 4. For a given ω, one can always find a continuum of $\hat{\alpha}$ such that there is a solution to (2.15) with constant-amplitude oscillations at either or both boundaries. Lees & Lin gave a physical interpretation of this pair of incoming and outgoing waves as an incoming wave and its reflection from the shear layer. Mack (1975) also used this idea in developing a theory for the forced response of the compressible boundary layer. We will ignore these continuum modes in the remainder of this paper.

One can now see that the appropriate boundary condition for either damped or outgoing waves in the moving and stationary streams are, respectively,

$$\hat{\Pi} \to \exp[-\Omega_+ \eta] \quad \text{if } c_r > c_+, \qquad \hat{\Pi} \to \exp[-i\eta(-\Omega_+^2)^{\frac{1}{2}}] \quad \text{if } c_r < c_+, \tag{2.22a}$$

$$\hat{\Pi} \to \exp[\Omega_- \eta] \quad \text{if } c_r < c_-, \qquad \hat{\Pi} \to \exp[-i\eta(-\Omega_-^2)^{\frac{1}{2}}] \quad \text{if } c_r > c_-. \tag{2.22b}$$

To solve the disturbance equation (2.15), we first transform it to a Riccati equation by setting

$$G = \frac{\hat{\Pi}'}{\hat{\alpha} T \hat{\Pi}}. \tag{2.23}$$

Thus, (2.15) becomes

$$G' + \hat{\alpha} T G^2 - \left[\frac{2U'}{U-c} - \frac{T'}{T}\right] G = \hat{\alpha}[T - \hat{M}^2 (U-c)^2]. \tag{2.24}$$

The boundary conditions can be found from (2.22) and (2.23).

The stability problem is thus to solve (2.24) for a given real frequency ω, Mach

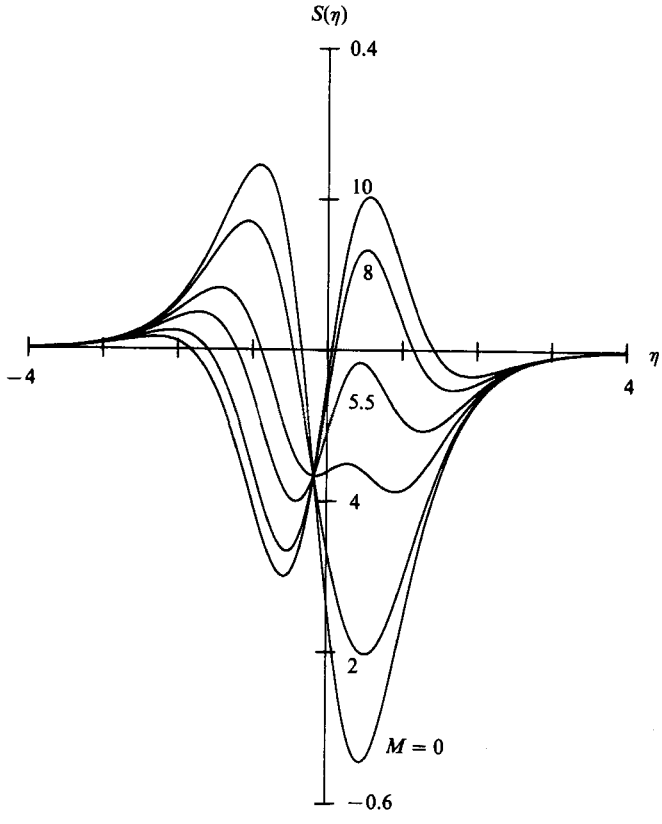

FIGURE 2. Plot of $S(\eta)$ for $\beta_T = 0.5$ and for various M.

number M, and angle of propagation θ, with U and T defined by (2.5) and (2.8). The eigenvalue is the wavenumber $\hat{\alpha}$. Because this equation has a singularity at $U = c_N$, we integrate it along the complex contour $(-6, -1)$ to $(0, -1)$ and $(6, -1)$ to $(0, -1)$ using a Runge–Kutta scheme with variable step size. We choose an initial $\hat{\alpha}$ and compute the boundary conditions from (2.22). We then iterate on $\hat{\alpha}$, using Muller's method, until the boundary conditions are satisfied and the jump in G at $(0, -1)$ is less than 10^{-6}. All calculations were done in 64-bit precision.

3. Results

In all of our calculations we have taken $\gamma = 1.4$, $\beta_T = \frac{1}{2}, 1, 2$, and $0 \leqslant M \leqslant 10$.

For a given real ω the wavenumber, $\hat{\alpha}$, must be real for a neutral mode. If $\hat{\alpha} = 0$, we require that $\hat{\Pi} \rightarrow$ constant at both boundaries. It can be shown that the corresponding phase speed is c_+, defined by (2.20), and that there are eigensolutions to (2.24) with this boundary condition.

Lees & Lin (1946) have proven that if a neutral mode is to exist in region 1, the phase speed will be given by $c_N = U(\eta_c)$, where η_c is found from the regularity condition

$$S(\eta) \equiv \frac{\mathrm{d}}{\mathrm{d}\eta}\left(T^{-2}\frac{\mathrm{d}U}{\mathrm{d}\eta}\right) = 0. \tag{3.1}$$

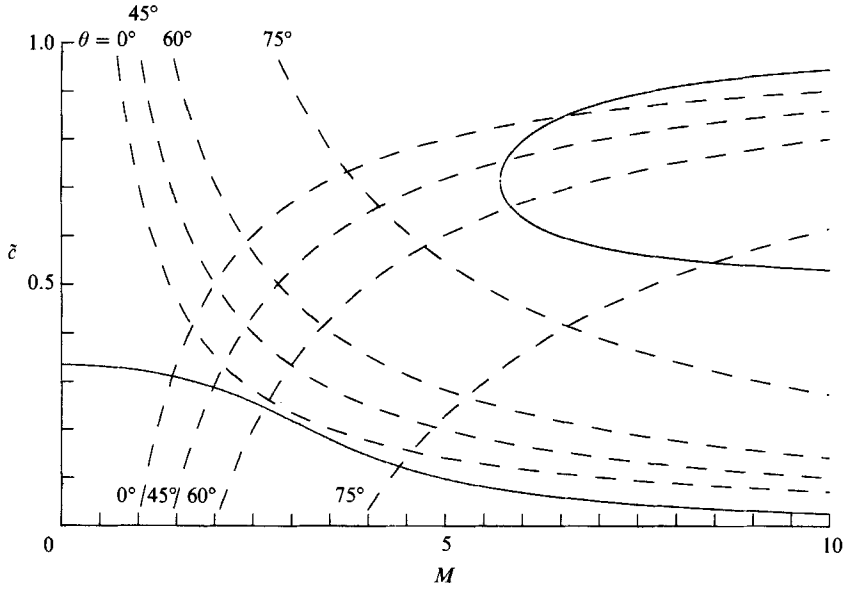

FIGURE 3. Plot of the real roots of $S, \tilde{c}$ (solid curve), versus Mach number for $\beta_T = 0.5$. Sonic curves, $c_\pm$ (dashed curves), are also shown for various propagation angles.

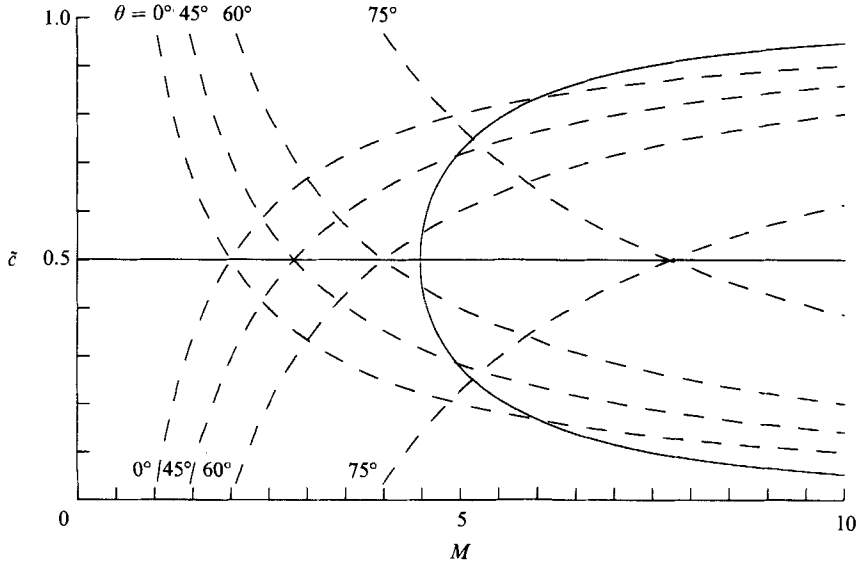

FIGURE 4. Plot of the real roots of $S, \tilde{c}$ (solid curve), versus Mach number for $\beta_T = 1$. Sonic curves, $c_\pm$ (dashed curves), are also shown for various propagation angles.

The corresponding neutral wavenumber, $\hat{\alpha}_N$, must be determined numerically. The eigenfunction is called a subsonic neutral mode. This result was obtained for the compressible boundary layer but it is easy to extend it to a mixing layer. This criterion has been used by Lessen *et al.* (1965) and Gropengiesser (1969) to find the phase speed of the subsonic neutral modes. Note that (3.1) differs from that given by

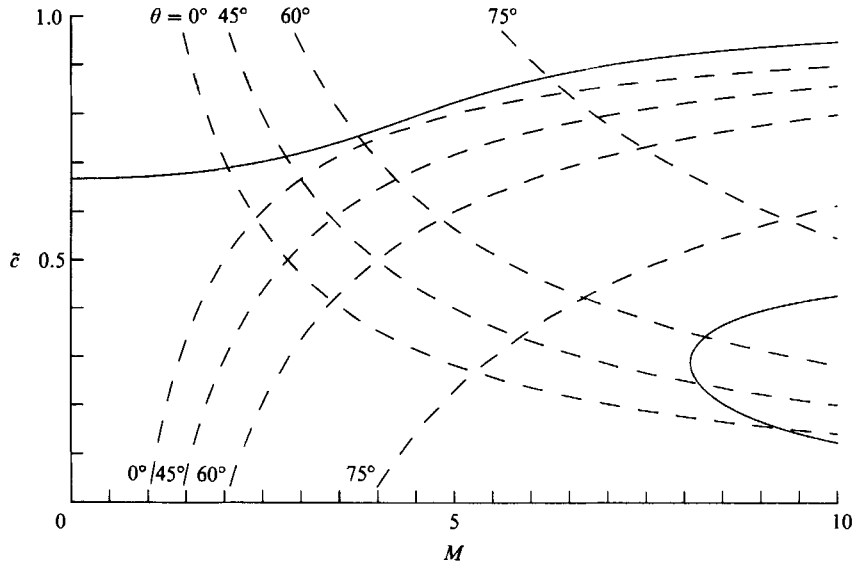

FIGURE 5. Plot of the real roots of $S, \tilde{c}$ (solid curve), versus Mach number for $\beta_T = 2$. Sonic curves, $c_\pm$ (dashed curves), are also shown for various propagation angles.

Lees & Lin, Lessen *et al.* and Gropengiesser by a factor of T^{-1} because they wrote (3.1) in terms of y and we have chosen to write it in terms of η.

The function $S(\eta)$ is a cubic when U and T are given by (2.5) and (2.8). Explicitly, one finds

$$Z^3 - aZ + b = 0, \tag{3.2}$$

with
$$a = 1 - \frac{4(1+\beta_T)}{(\gamma-1)M^2}, \quad b = \frac{4(1-\beta_T)}{(\gamma-1)M^2}, \tag{3.3}$$

where
$$Z \equiv \tanh(\eta). \tag{3.4}$$

Thus, if Z is a root of (3.2), the phase speed of a possible neutral mode is

$$\tilde{c} = \tfrac{1}{2}(1+Z). \tag{3.5}$$

Equation (3.2) has either one or three real roots with at least two of the three real roots equal if the discriminant is zero. If we define M_0 by

$$M_0 = 2(\gamma-1)^{-\frac{1}{2}}\{1+\beta_T+\tfrac{3}{2}(1-\beta_T)^{\frac{2}{3}}[(1+\beta_T^{\frac{1}{2}})^{\frac{2}{3}}+(1-\beta_T^{\frac{1}{2}})^{\frac{2}{3}}]\}^{\frac{1}{2}}, \tag{3.6}$$

then there is one real root for $M < M_0$ and three real roots for $M \geqslant M_0$. In particular, as $M \to 0$, only one real root exists and is given by

$$Z = \frac{(\beta_T - 1)}{(\beta_T + 1)}, \tag{3.7}$$

with corresponding phase speed

$$\tilde{c} = \frac{\beta_T}{(1+\beta_T)}. \tag{3.8}$$

Also, as $M \to \infty$, there are now three roots $Z = -1, 0, 1$, giving $\tilde{c} = 0, \frac{1}{2}, 1$, respectively.

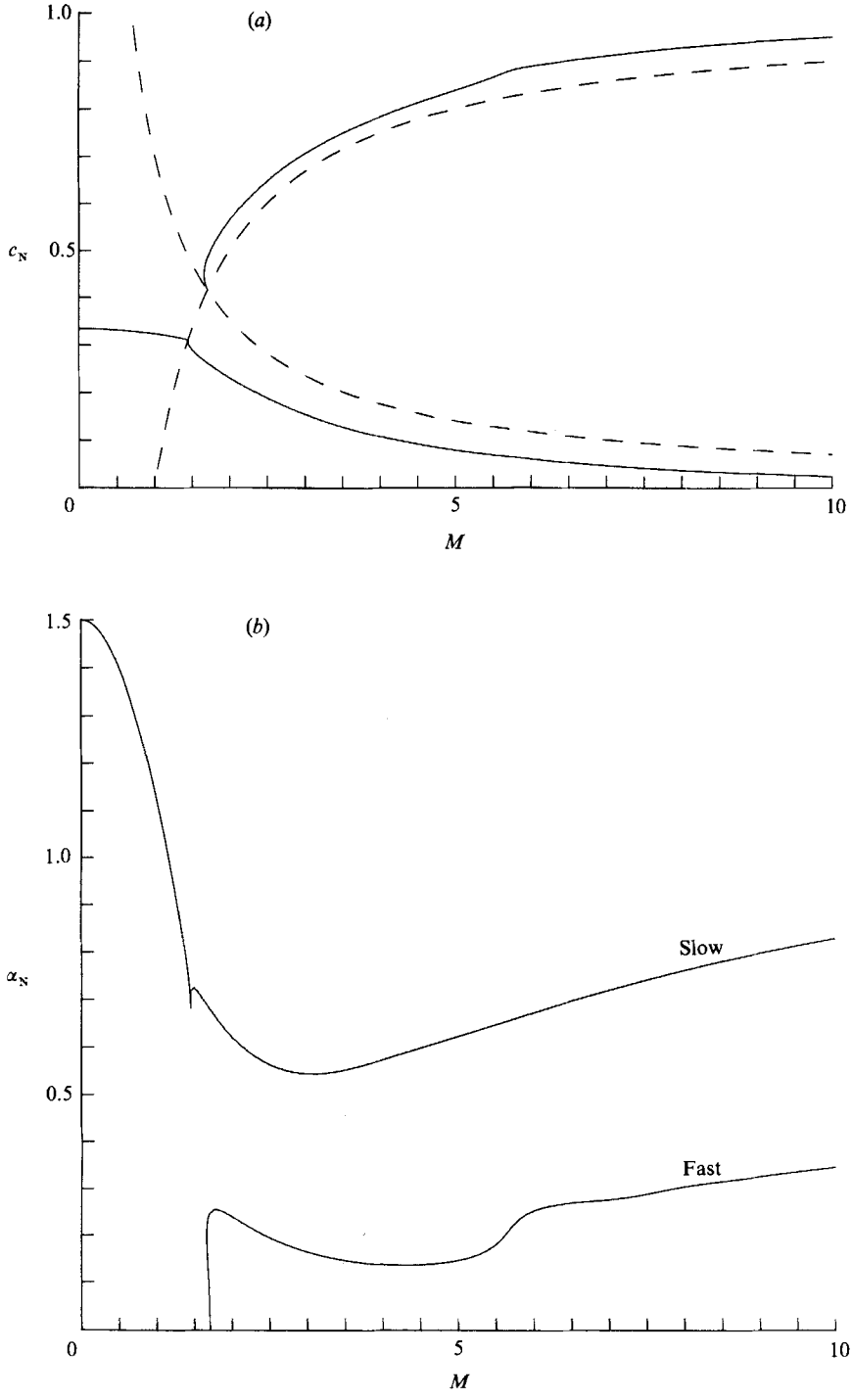

FIGURE 6(a, b). For caption see facing page.

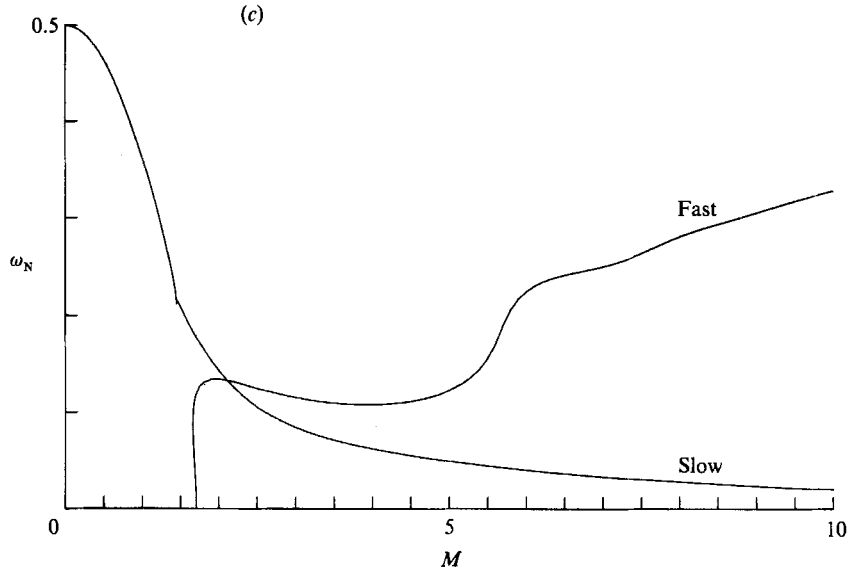

FIGURE 6. Plots of two-dimensional neutral curves for $\beta_T = 0.5$ versus Mach number: (*a*) phase (solid) and sonic (dashed) speeds; (*b*) wavenumbers of the fast and slow modes; (*c*) frequencies of the fast and slow modes.

Recall that the phase speed of a possible neutral mode is given by (3.5) for each real root. The theorem of Lees & Lin ensures that this is in fact a neutral mode if the wave speed of the mode lies in region 1, and hence $\tilde{c} = c_N$. If a root of (3.2) yields a phase speed which lies in regions 2, 3, or 4, it may, or may not, be a true neutral mode propagating away from the mixing layer. One must determine whether or not, for this phase speed, there is an outgoing solution of (2.24) which satisfies the appropriate boundary conditions.

We, of course, solve for the roots of (3.2) directly but insight can be gained by plotting $S(\eta)$ over a range of values of η for various values of M and fixed β_T. Figure 2 is a plot of $S(\eta)$ versus η for $\beta_T = 0.5$ and $M = 0, 2, 4, 5.5, 8, 10$. One sees that, for $M < M_0 = 5.715$, the single real root of (3.2) gives a $\tilde{c} < \frac{1}{2}$; that is the 'critical point' is at some $\eta < 0$. However, if $M > M_0$, there are three real roots with one at $\eta < 0$ and the other two at $\eta > 0$.

Gropengiesser stated that if $\beta_T < 0.6$ and $M > 3$, $S(\eta)$ had three zeros. On closer examination, the results shown in his figure 7 suggest that there will always be three zeros for high enough Mach numbers. He was able to find a neutral solution which satisfied the boundary conditions for only one of these three values and hence ignored the other two zeros of S. It must be noted that Gropengiesser only considered two-dimensional disturbances in reaching this conclusion.

Figures 3, 4, and 5 are plots of the real roots of S, $\tilde{c}$, from (3.5) as a function of the Mach number and for $\beta_T = \frac{1}{2}, 1, 2$, respectively. These figures show that the real zeros of S yield a monotonic curve and a 'bubble'. It is easy to show that this surface has a saddle point at $\beta_T = 1$ and $M = [8/(\gamma-1)]^{\frac{1}{2}}$. The sonic curves $c_\pm$ are also plotted for three-dimensional waves with propagation angles of 0°, 45°, 60°, 75°.

We have carried out numerical calculations in order to determine whether or not the zeros of S always yield the phase speed of a neutral mode. We find, in agreement

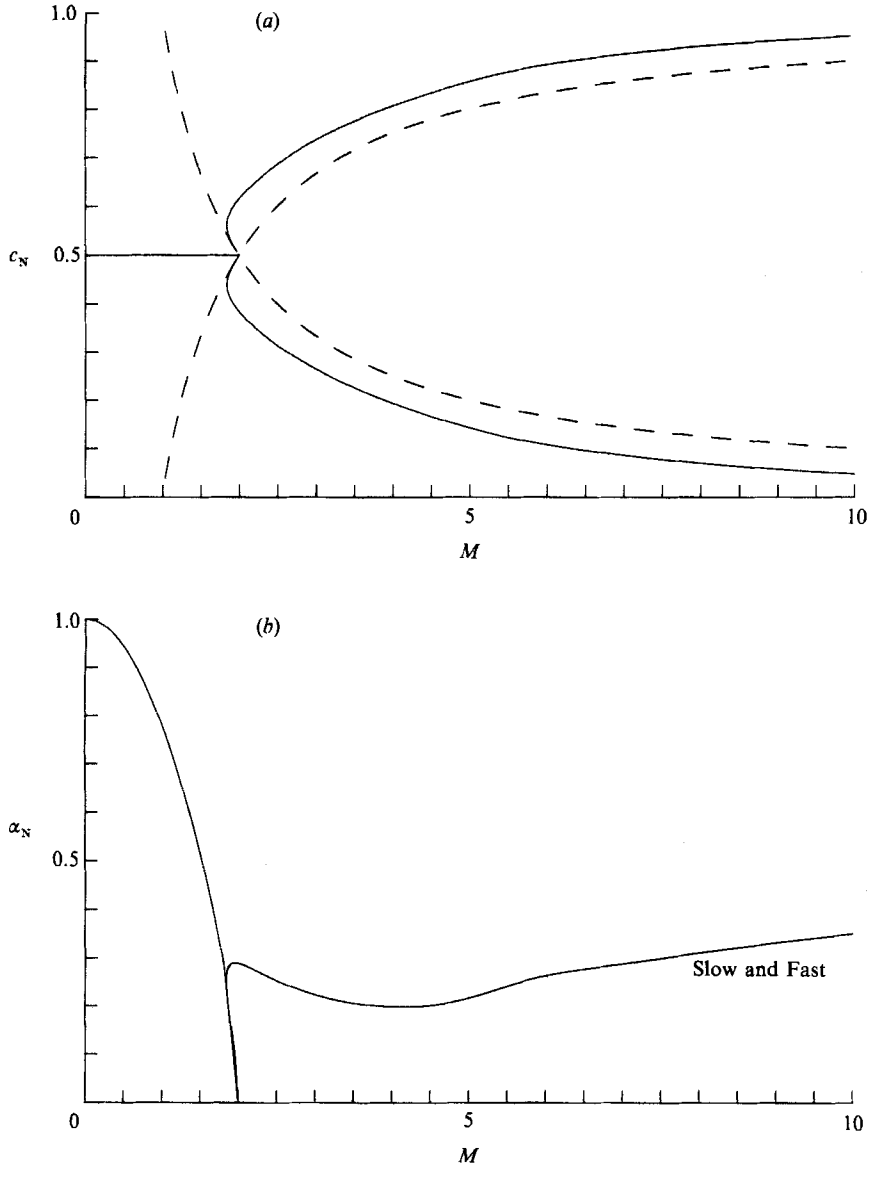

FIGURE 7(a, b). For caption see facing page.

with Gropengiesser, Lessen *et al.* and Lees & Lin, that such is the case only if the solution is subsonic at both boundaries, i.e. it lies in region 1. Gropengiesser concluded that only one of the zeros of S gave the phase speed of a true neutral mode. This is true only if the mode is two-dimensional. One can see from figures 3–5 that, for any β_T, if the mode is two-dimensional ($\theta = 0°$) there is only one zero of S in region 1. We find that there is a neutral mode corresponding to this value of $\tilde{c}$. For the other zeros of S, we find that there are no solutions which yield damped or outgoing waves if $\theta = 0°$. However, the sonic speeds $c_\pm$ are functions of the angle of propagation. As θ increases the sonic curves shift towards higher Mach number. Thus for any value of β_T, there will always be some angle of propagation for which all three

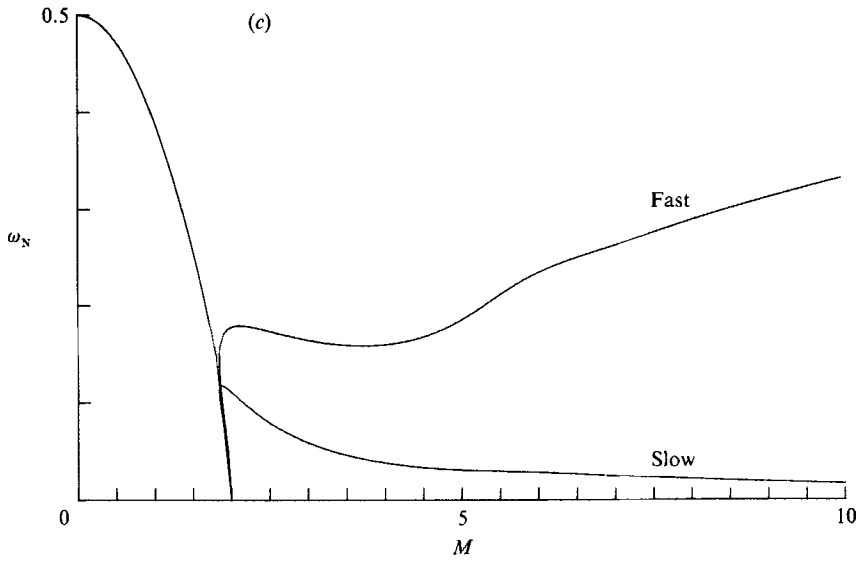

FIGURE 7. Plots of two-dimensional neutral curves for $\beta_T = 1$ versus Mach number: (*a*) phase (solid) and sonic (dashed) speeds; (*b*) wavenumbers of the fast and slow modes; (*c*) frequencies of the fast and slow modes.

zeros of S lie in region 1. For example, in figure 4, if $\theta > 63.44°$, all three zeros of S can correspond to modes which are subsonic at both boundaries. Hence, by the theorem of Lees & Lin, there are now three neutral modes with phase speeds equal to the value of U at the corresponding values of η_c. Thus, the significance of the three real zeros of S only becomes apparent at very large angles of propagation.

There can also be supersonic neutral modes: those which do not satisfy (3.1) but are solutions of (2.24) with only outgoing or damped waves at $\pm\infty$. It is obvious that these are singular eigenfunctions. The singularity will be removed by the action of non-zero viscosity. Hence we can regard these singular modes as the limit of some viscous, spatial stability modes as the Reynolds number approaches infinity.

One can find these modes by obtaining numerical solutions of (2.24) which are either decaying (if the disturbance is subsonic) or outwardly propagating (if the disturbance is supersonic) at $\pm\infty$, without requiring that (3.1) be satisfied. We have carried out such calculations and found that, for any value of β_T, there is always one supersonic neutral mode in region 2 of the (c_r, M)-plane and another supersonic neutral mode in region 4.

Results for the two-dimensional neutral modes are shown in figures 6, 7, and 8. Figures 6(*a*), 7(*a*) and 8(*a*) are plots of the neutral phase speed c_N as a function of the Mach number and for $\beta_T = \frac{1}{2}$, 1, 2, respectively. The dashed curves are the neutral sonic modes with phase speeds $c_\pm$ and $\hat{\alpha} = 0$. For each value of β_T there is a single subsonic neutral wave in region 1. As M is increased, this subsonic mode crosses over the sonic curve at M_s, the Mach number at which the phase speed equals that of a sonic wave, into either region 2 or 4 and is transformed into a supersonic neutral mode. If $\beta_T > 1$, this mode becomes a fast mode whose phase speed approaches 1 as M goes to infinity. If $\beta_T < 1$, the mode becomes a slow mode whose phase speed approaches zero as the Mach number increases. In each case, there is also another supersonic neutral mode, fast if $\beta_T < 1$ and slow if $\beta_T > 1$. These modes, which have

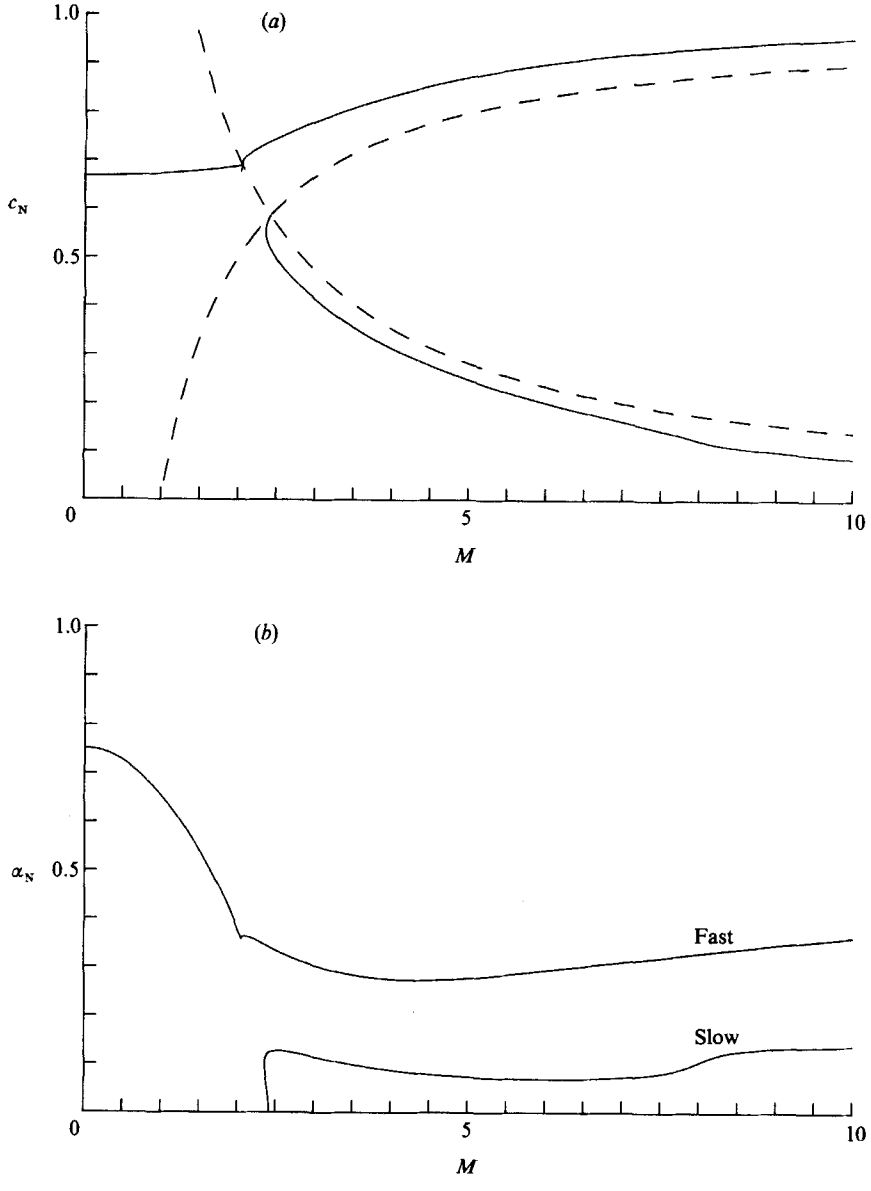

FIGURE 8(a, b). For caption see facing page.

non-zero frequency, appear as M_* where the phase speeds are equal to the sonic speeds. If $\beta_T = 1$, the subsonic mode splits symmetrically into a fast and a slow supersonic wave. Note that for a small range of M around M_* there can be more than three different neutral modes in addition to the two sonic modes.

The corresponding wavenumbers, displayed in figures 6(b)–8(b), decrease as the Mach number increases from 0 to M_s. The mode with the larger wavenumber is always the subsonic mode and its supersonic continuation at higher Mach numbers. The other mode always has a smaller wavenumber and hence a longer wavelength. The discontinuity in the slope of the wavenumber curves is due to the transformation from a subsonic to a supersonic mode when crossing a sonic curve. This is because the

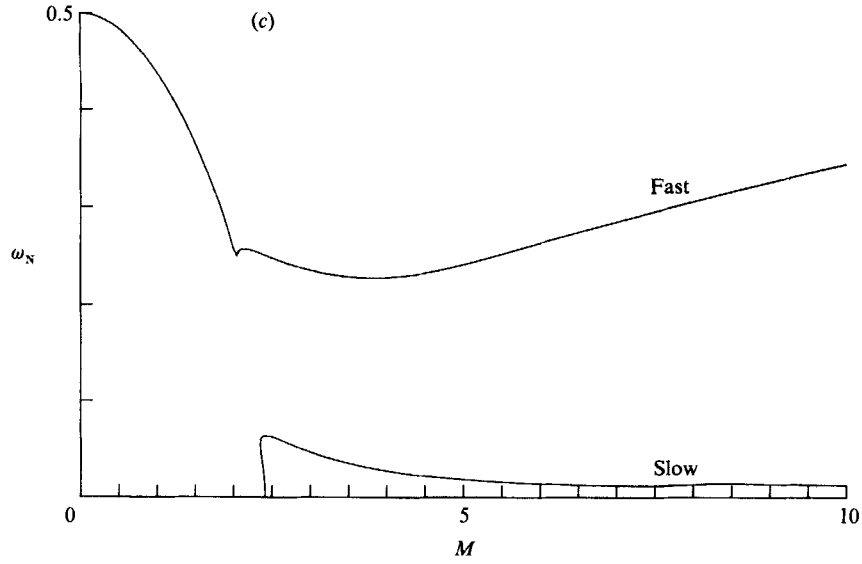

FIGURE 8. Plots of two-dimensional neutral curves for $\beta_T = 2.0$ versus Mach number: (*a*) phase (solid) and sonic (dashed) speeds; (*b*) wavenumbers of the fast and slow modes; (*c*) frequencies of the fast and slow modes.

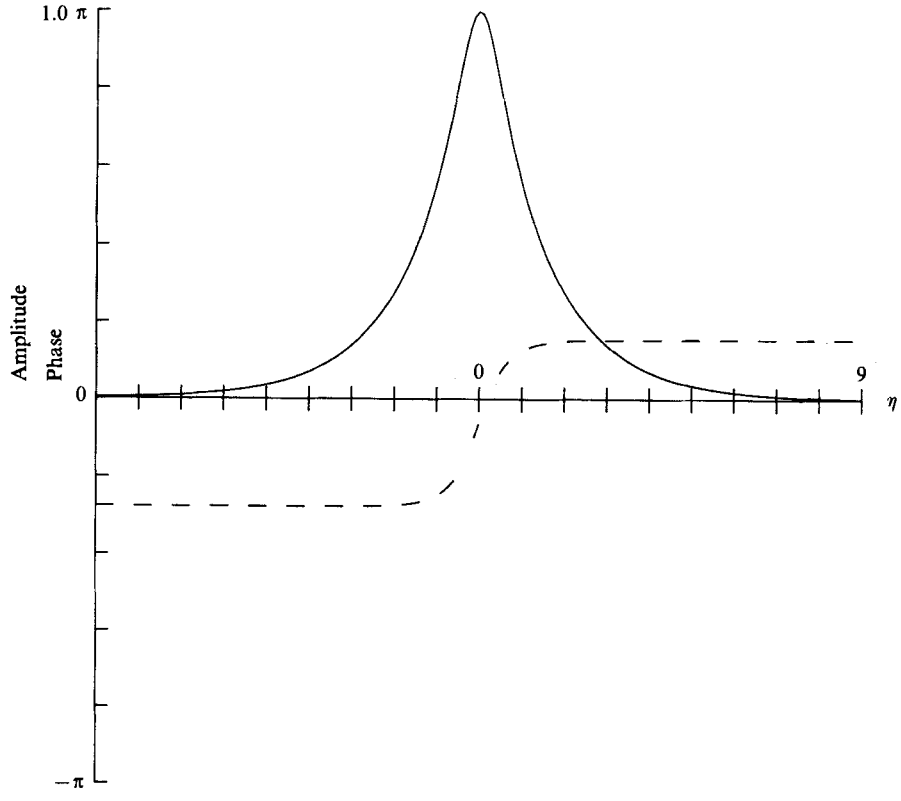

FIGURE 9. Plot of the two-dimensional subsonic neutral eigenfunction $\Pi(\eta)$ along the contour $\eta = \eta_r - \mathrm{i}$. The solid curve corresponds to the amplitude and the dashed curve to the phase. $M = 1$, $\beta_T = 1$, $\omega_N = 0.390495$, $\alpha_N = 0.780991$, $c_N = 0.5$.

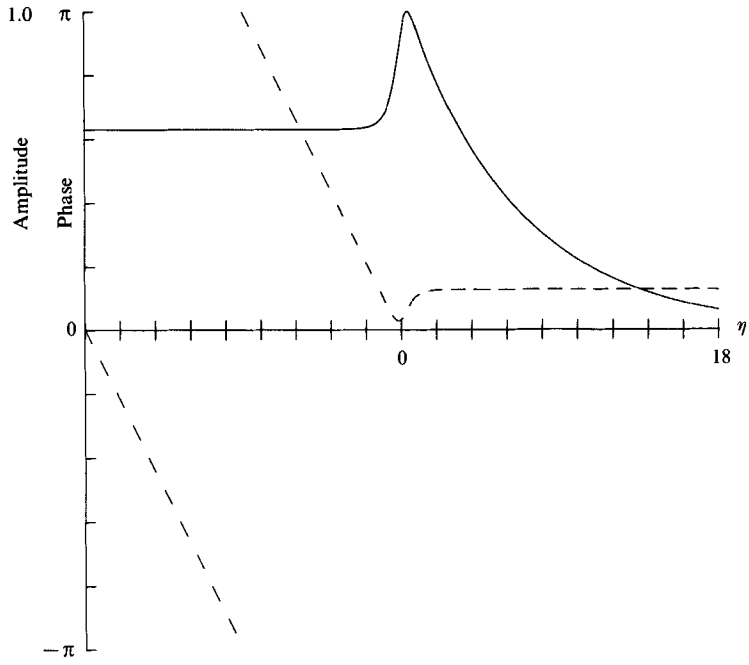

FIGURE 10. Plot of the two-dimensional fast supersonic neutral eigenfunction $\Pi(\eta)$ along the contour $\eta = \eta_r - i$. The solid curve corresponds to the amplitude and the dashed curve to the phase. $M = 2.5$, $\beta_T = 1$, $\omega_N = 0.173064$, $\alpha_N = 0.252214$, $c_N = 0.68618$.

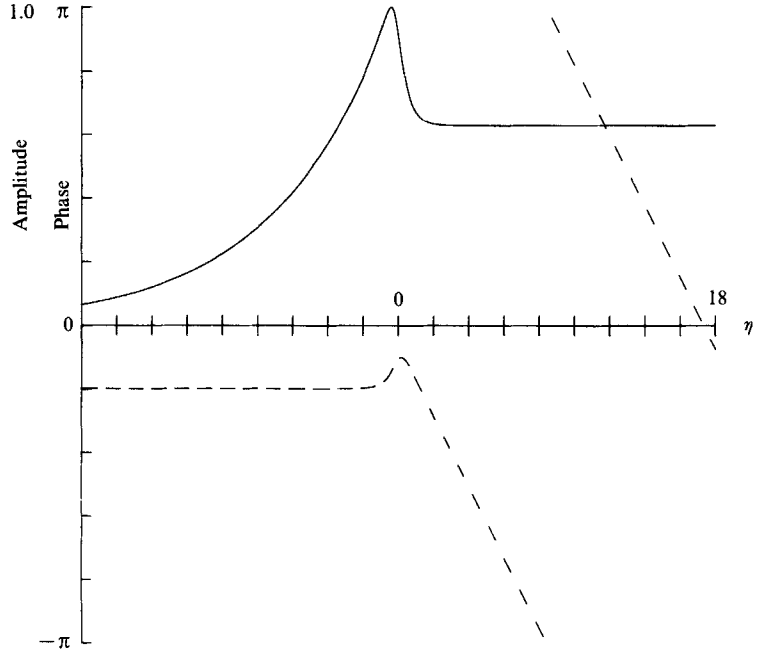

FIGURE 11. Plot of the two-dimensional slow supersonic neutral eigenfunction $\Pi(\eta)$ along the contour $\eta = \eta_r - i$. The solid curve corresponds to the amplitude and the dashed curve to the phase. $M = 2.5$, $\beta_T = 1$, $\omega_N = 0.079151$, $\alpha_N = 0.252214$, $c_N = 0.31382$.

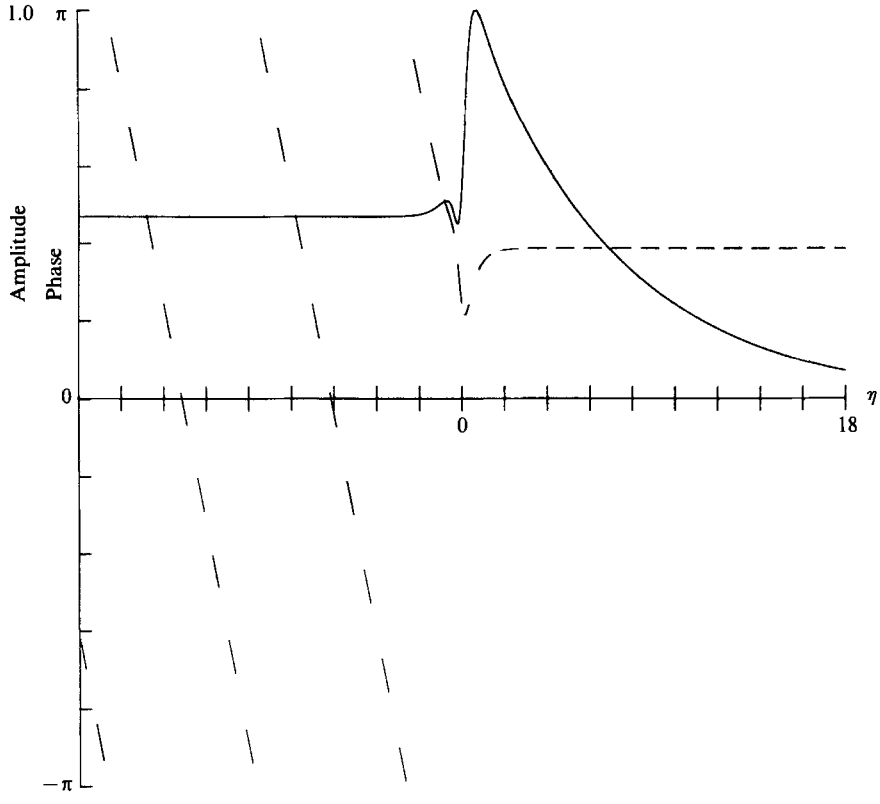

FIGURE 12. Plot of the two-dimensional fast supersonic neutral eigenfunction $\Pi(\eta)$ along the contour $\eta = \eta_r - \mathrm{i}$. The solid curve corresponds to the amplitude and the dashed curve to the phase. $M = 5$, $\beta_T = 1$, $\omega_N = 0.184813$, $\alpha_N = 0.215661$, $c_N = 0.85696$.

character of the supersonic neutral mode is singular and that of the subsonic neutral mode is regular. Thus, the limit of the slopes of their respective wavenumber curves at the sonic point need not be equal. For $\beta_T = 1$, both the fast and slow supersonic waves have the same value of the wavenumber at any $M > M_s = M_*$. For all β_T, the wavenumbers increase slightly with Mach number.

Finally, the corresponding frequencies, displayed in figures 6(*c*)–8(*c*), decrease as the Mach number increases from 0 to M_s. For $M > M_*$, the frequency of one of the supersonic modes increases and that of the other decreases. This, combined with the relatively constant values of the wavenumbers, leads to the appearance of fast and slow modes. If $\beta_T < 1$, the curves of ω_N for the supersonic modes must cross at some $M > M_*$. Thus, one will have two different neutral modes at the same frequency and Mach number but with different wavenumbers. If $\beta_T > 1$ the neutral modes have quite different frequencies.

Based on our numerical results, we find that for $M = 0$,

$$c_N = \frac{\beta_T}{(1+\beta_T)}, \quad \alpha_N = \frac{1+\beta_T}{2\beta_T}\cos(\theta), \quad \omega_N = \tfrac{1}{2}\cos(\theta), \tag{3.9}$$

consistent with (3.8) and figures 6–8.

Figures 9–13 are plots of selected two-dimensional neutral eigenfunctions for

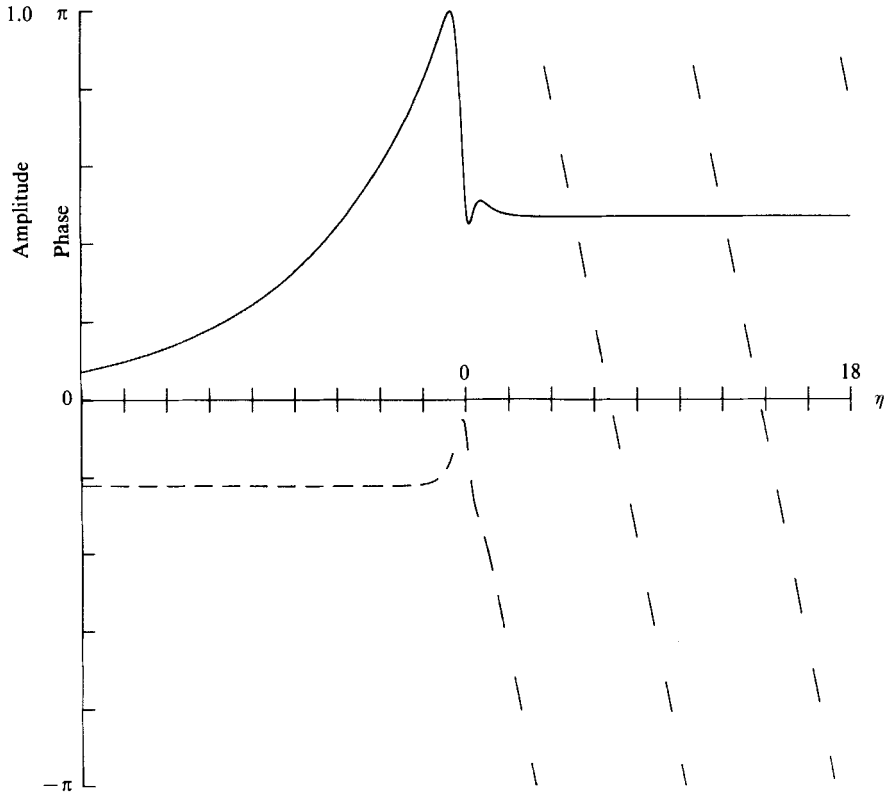

FIGURE 13. Plot of the two-dimensional slow supersonic neutral eigenfunction $\Pi(\eta)$ along the contour $\eta = \eta_r - \mathrm{i}$. The solid curve corresponds to the amplitude and the dashed curve to the phase. $M = 5$, $\beta_T = 1$, $\omega_N = 0.030847$, $\alpha_N = 0.215661$, $c_N = 0.14303$.

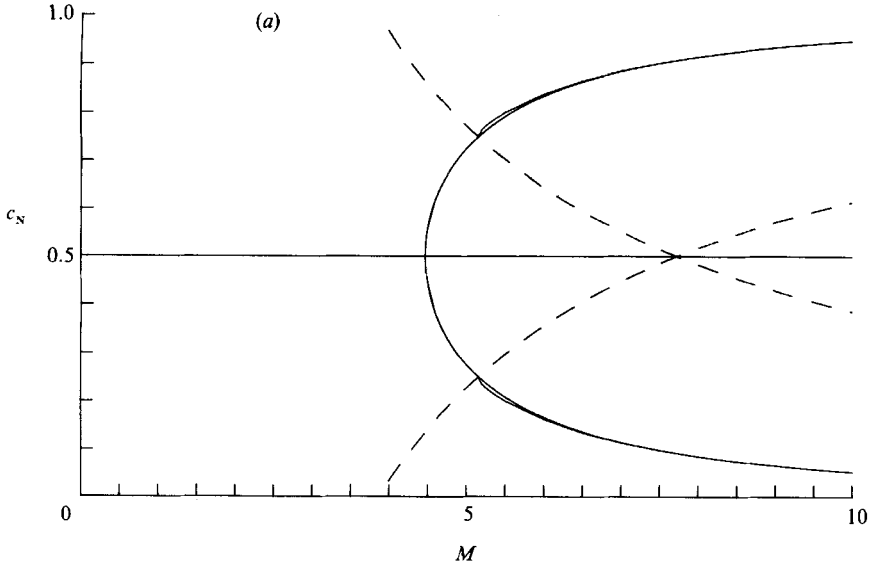

FIGURE 14(a). For caption see facing page.

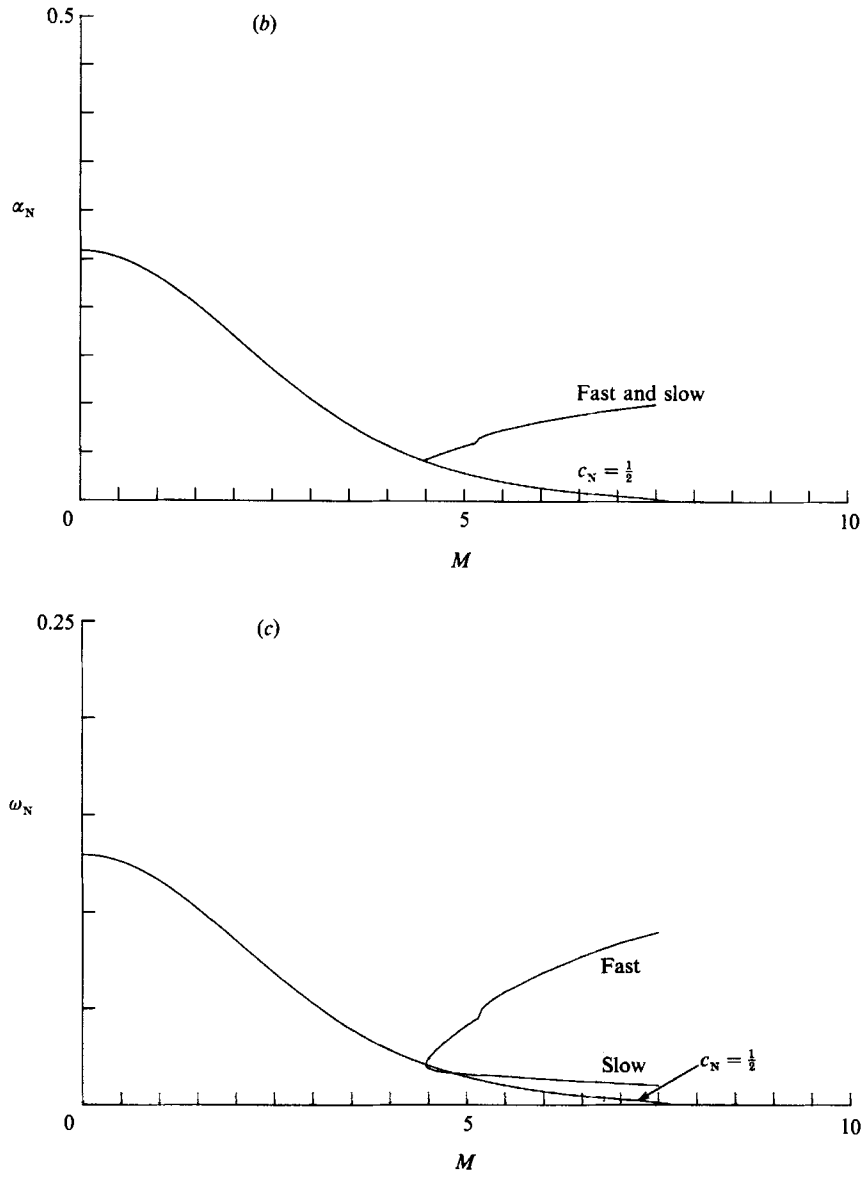

FIGURE 14. Plot of three-dimensional ($\theta = 75°$) neutral curves for $\beta_T = 1$ versus Mach number: (*a*) phase (solid) and sonic (dashed) speeds; (*b*) wavenumbers; (*c*) frequencies; all of the fast, slow, and continuation of $c_N = \frac{1}{2}$ modes.

$\beta_T = 1$. These plots show the variation of Π with η_r on the contour $\eta_i = -1$. All of these have been normalized so that the maximum of the absolute value of Π is unity. The eigenfunction shown in figure 9 is a subsonic neutral mode at $M = 1$. The wave is subsonic at both boundaries, so Π decays exponentially away from the mixing layer. Note the rapid variation of the phase near $\eta_r = 0$. Figures 10 and 11 are plots of the two fast and slow supersonic neutral waves of Π at $M = 2.5$. The eigenvalue for the eigenfunction in figure 10 lies in region 2 so the fast wave is subsonic at $+\infty$ and supersonic at $-\infty$. The eigenvalue for the slow wave shown in figure 11 lies in

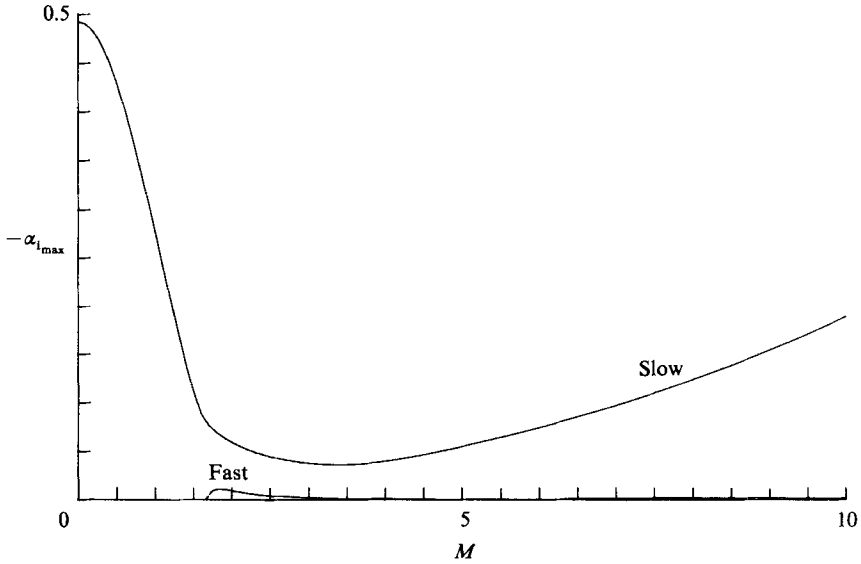

FIGURE 15. Plot of maximum growth rate of the fast and slow two-dimensional modes versus Mach number for $\beta_T = 0.5$.

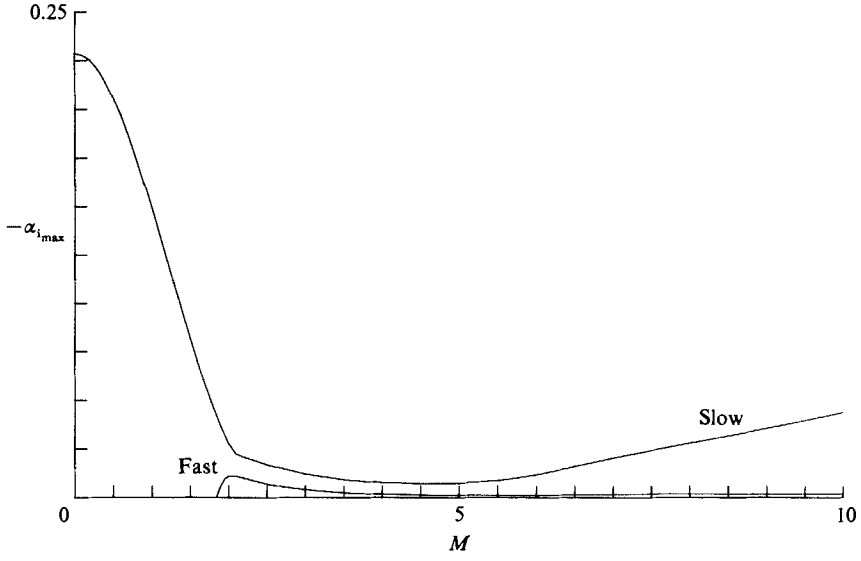

FIGURE 16. Plot of maximum growth rate of the fast and slow two-dimensional modes versus Mach number for $\beta_T = 1$.

region 4 and has just the opposite behaviour. Both modes show exponential decay in the subsonic region and oscillations with constant amplitude and linear phase in the supersonic region. Both show a rapid phase shift near the centre of the mixing layer. Finally, figures 12 and 13 are plots of the supersonic neutral eigenfunctions at $M = 5$. As before, the eigenvalue of the fast wave of figure 12 lies in region 2 and that of the slow wave of figure 13 in region 4. The behaviour of these eigenfunctions is quite similar to that of the modes at $M = 2.5$, but note that the wavelength of the oscillation decreases as the Mach number increases.

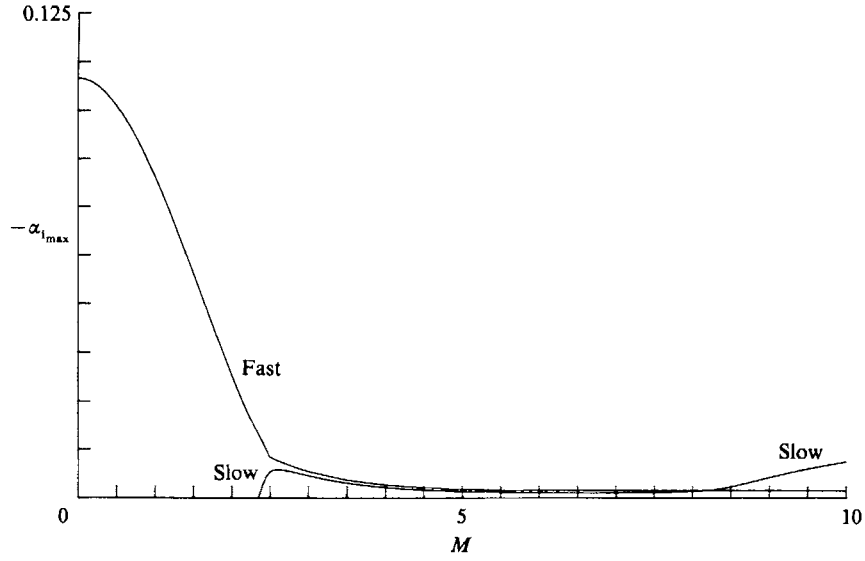

FIGURE 17. Plot of maximum growth rate of the fast and slow two-dimensional modes versus Mach number for $\beta_T = 2$.

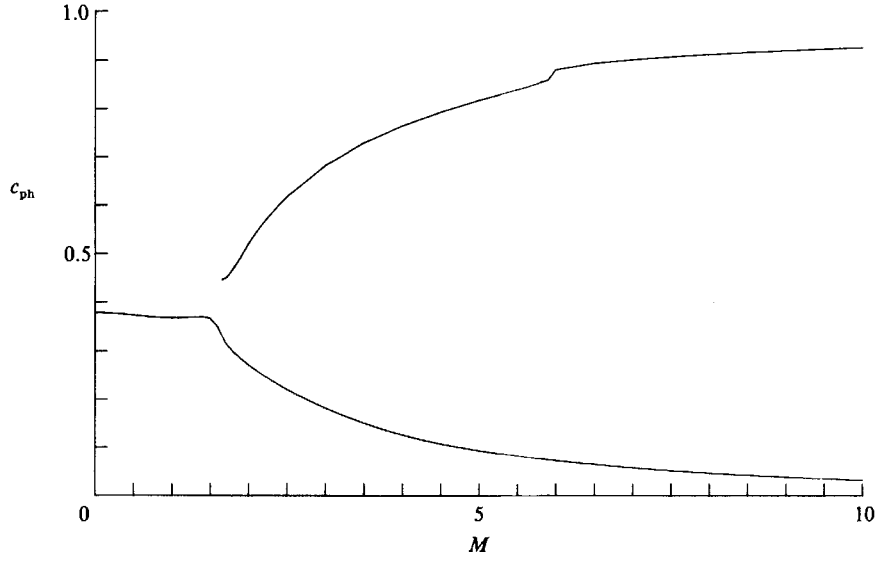

FIGURE 18. Plot of phase speeds c_{ph} of the most rapidly growing fast and slow two-dimensional modes versus Mach number for $\beta_T = 0.5$.

As was stated above all three real roots of S can be the phase speeds of subsonic neutral modes if the disturbance wave is three-dimensional. As an example, we show in figure 14 results for the neutral modes at $\beta_T = 1$ and $\theta = 75°$. From $M = 0$ up to $M_0 = 4.472$ there is a single subsonic neutral mode with $c_N = 0.5$ and both α_N and ω_N monotonically decreasing. For $M \geqslant M_0$, S has three real roots and these are the phase speeds of the three subsonic neutral modes for $M_0 \leqslant M \leqslant 5.15$. One of these modes has $c_N = 0.5$, another has an increasing c_N and the other a decreasing c_N. From figures

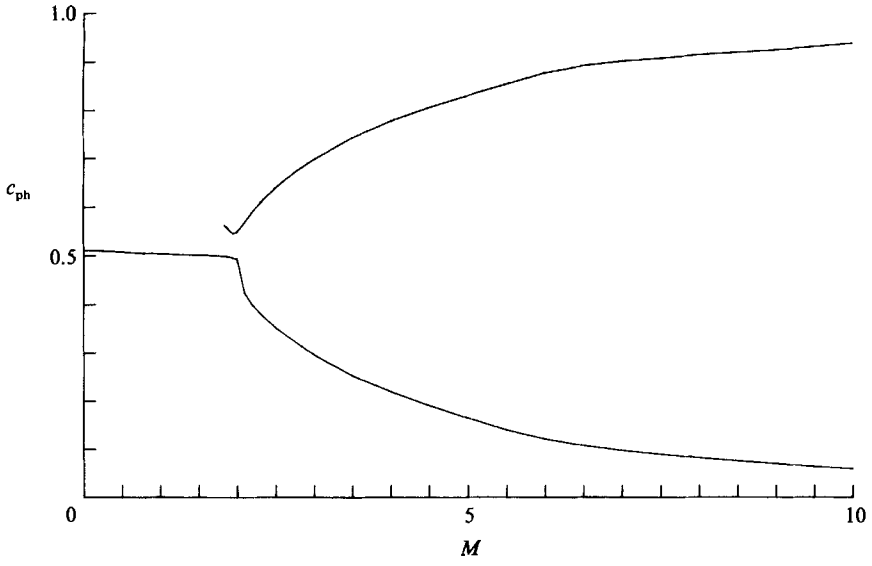

FIGURE 19. Plot of phase speeds c_{ph} of the most rapidly growing fast and slow two-dimensional modes versus Mach number for $\beta_T = 1$.

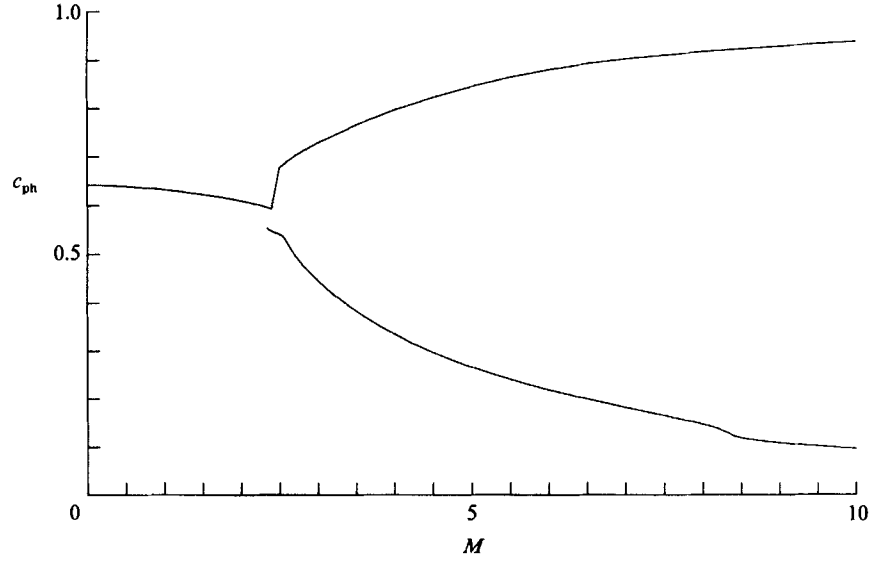

FIGURE 20. Plot of phase speeds c_{ph} of the most rapidly growing fast and slow two-dimensional modes versus Mach number for $\beta_T = 2$.

14(*b*) and 14(*c*) one can see that α_N and ω_N for the mode $c_N = 0.5$ decrease monotonically until they vanish at $M_* = 7.727$. The wavenumbers of the other two neutral waves increase with M beyond M_0. The curves of α_N for these modes show a discontinuity in slope at $M_s = 5.15$ as they intersect the sonic curves and are transformed into supersonic neutral modes. The phase speeds of these supersonic modes are only slightly different from, and appear to be asymptotic to, the values obtained from the zeros of S. Finally, the curves of ω_N split at M_0 with that of the

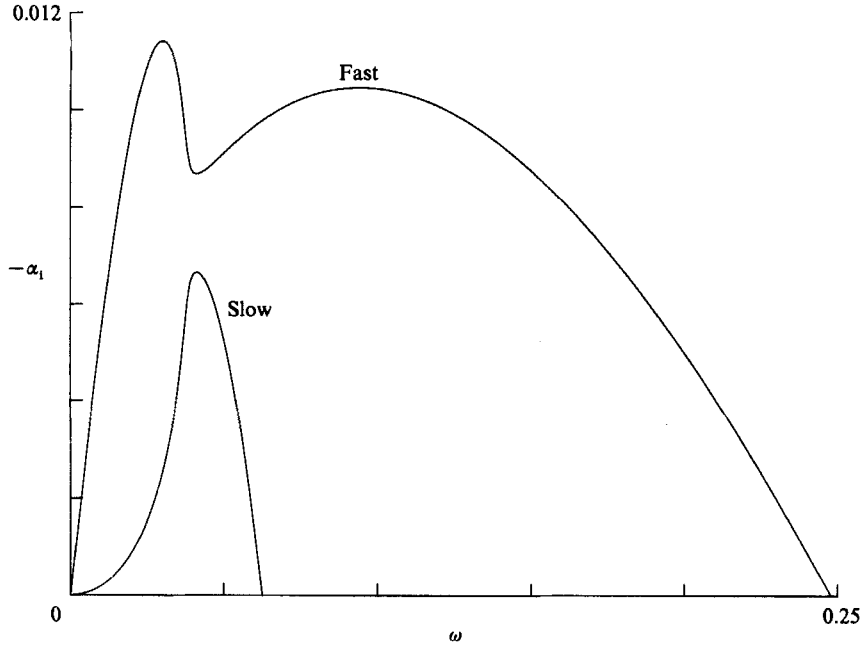

FIGURE 21. Plot of growth rates α_i of the fast and slow two-dimensional modes versus frequency for $\beta_T = 2$ and $M = 2.5$.

fast mode increasing and that of the slow mode decreasing. These curves also show discontinuities in slope at $M_s = 5.15$.

We have carried out calculations to determine the growth rates of the unstable modes. Some of these results are shown in figures 15, 16, and 17 where we have plotted the maximum growth rate ($-\alpha_{i_{max}}$) for two-dimensional modes as a function of Mach number and for $\beta_T = \frac{1}{2}$, 1, 2, respectively. Each of these figures shows two curves. The curve giving the larger values of the growth rate is that of the first group of unstable waves, that group which exists for $M < M_*$. For $\beta_T \leqslant 1$ this group corresponds to the slow modes while for $\beta_T > 1$ it corresponds to the fast modes. The second curves gives the maximum growth rate for the group of unstable waves which appears at M_*. These are the fast modes for $\beta_T \leqslant 1$ and the slow modes for $\beta_T > 1$. In all cases there is a decrease in the maximum growth rate by a factor of five to ten as the Mach number approaches M_*. For Mach numbers greater than M_*, the growth rates level off and those of the slow modes begin to increase with increasing Mach number while those of the fast modes approach a limiting value. However, even at Mach 10, the growth rates are still small compared with those at low subsonic speeds. Finally, note that a decrease in β_T results in an increase in the growth rate of the unstable modes at any Mach number.

In figures 18–20 we plot the phase speeds c_{ph} of the most rapidly growing fast and slow two-dimensional modes versus Mach number for $\beta_T = \frac{1}{2}$, 1, 2, respectively. As would be expected the band of unstable waves is adjacent to the neutral modes for $M < M_s$. For $\beta_T \leqslant 1$, the most rapidly growing mode has a phase speed slightly greater than the corresponding neutral mode in this range, while for $\beta_T > 1$, the phase speed is slightly less than that of the neutral mode. For Mach numbers greater than M_s the most unstable mode has a phase speed which lies between the supersonic neutral curve and the sonic neutral curve. Note that for $\beta_T = 2$, there is a rapid

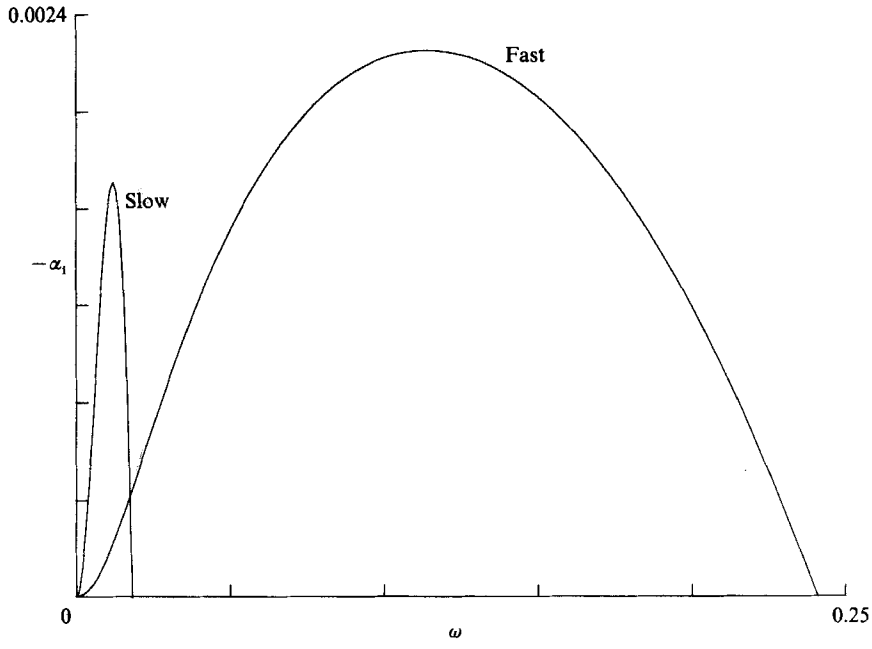

FIGURE 22. Plot of growth rates α_i of the fast and slow two-dimensional modes versus frequency for $\beta_T = 2$ and $M = 5$.

change in the phase speed of the fast mode around M_*. This is due to a shift in the frequency of the most unstable mode in this Mach number range.

In order to display the characteristics of both of these unstable waves in more detail we consider a single case, that of $\beta_T = 2$. The phase speed, wavenumbers, and frequencies of the neutral modes are shown in figure 8 and the maximum growth rates in figure 17. The slow supersonic group of unstable modes only exist for $M > M_* = 2.414$. Figure 21 is a plot of the growth rate versus frequency of the unstable two-dimensional modes at Mach 2.5. This value of M was chosen so as to be slightly above M_*. The upper curve is that of the fast waves. There are two neutral frequencies: $\omega_N = 0$ corresponds to the sonic mode c_+; and $\omega_N = 0.24$ corresponds to that of the fast supersonic neutral mode. From figure 8 one can see that the phase speeds of these modes lie in the range 0.6 to 0.745, suggesting that the wave packets of these modes would have modest dispersion. The upper curve has two maxima, one at $\omega = 0.025$ and the other at $\omega = 0.09$. These are nearly the same size, but that of the larger value of ω is much broader.

The growth rates for the slow supersonic modes are shown by the lower curve in figure 21. These slow waves have phase speeds between 0.494 and 0.566. The slow unstable modes have a maximum growth rate of about two-thirds of that of the fast modes. However, the band of unstable frequencies is much narrower for the slow modes than for the fast ones. The zero of the growth rate at $\omega_N = 0$ corresponds to the sonic curve c_- and the other zero to the slow supersonic neutral modes.

The results shown in figure 22 are similar to that of figure 21 but for Mach 5. The maximum growth rates of both groups of waves at Mach 5 are only about one-fifth of those at Mach 2.5. The fast modes exist over a frequency range about the same as at Mach 2.5, but the phase speeds all lie in the range of 0.8 to 0.873. The frequency band of the slow modes is much less at Mach 5 than at 2.5, and hence there is a shift

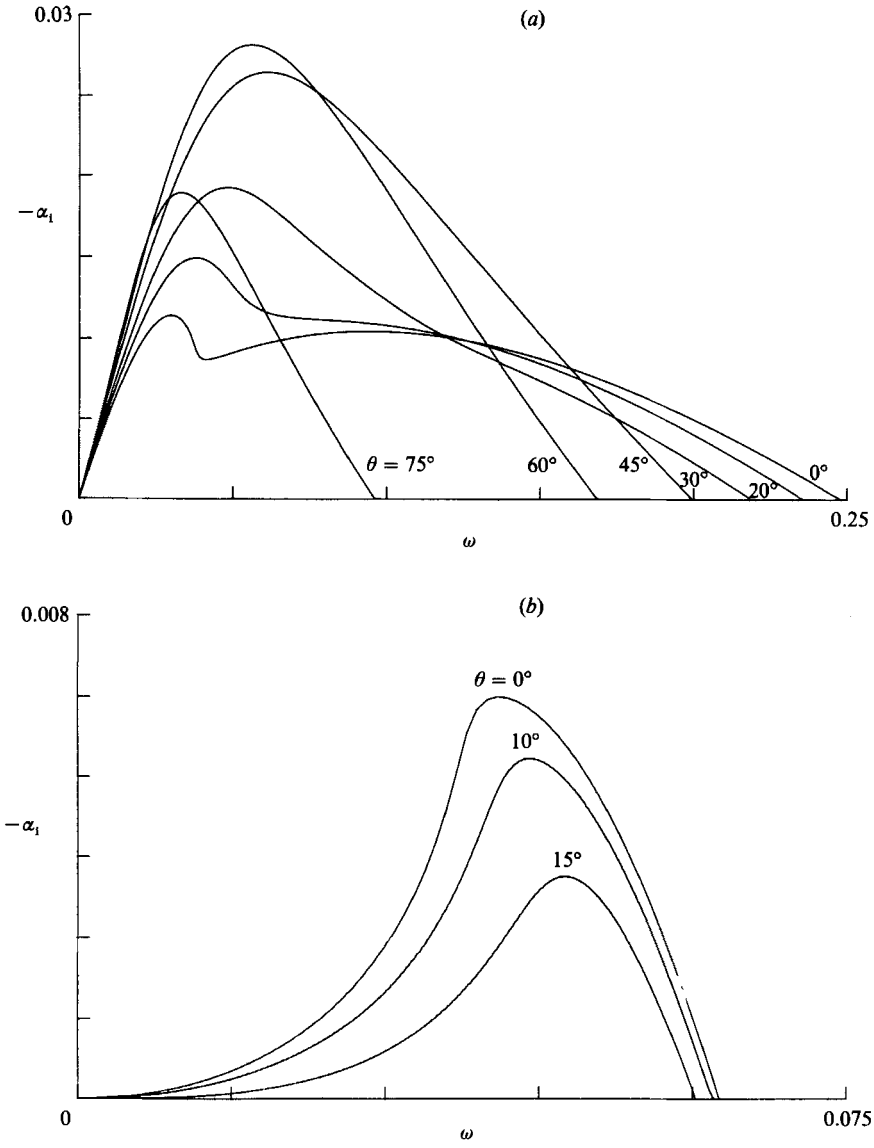

FIGURE 23. Plot of growth rates α_i for three-dimensional modes versus frequency for $\beta_T = 2$, $M = 2.5$: (*a*) fast modes; (*b*) slow modes.

in the frequency of maximum growth towards zero. Thus at Mach 2.5 the slow modes have their maximum growth rate at a higher frequency than the fast modes but this is reversed at Mach 5. The phase speeds of the slow modes are much different from those of the fast modes at this Mach number, ranging from 0.249 to 0.283. Since the range of phase speeds of both the fast and slow modes decreases as the Mach number increases, the amount of dispersion is reduced as the Mach number increases.

The results of figures 21 and 22 are for two-dimensional modes. The same general behaviour is also characteristic of three-dimensional waves. Figure 23(*a*) shows the growth rates of the fast modes and 23(*b*) the growth rates of the slow modes as a function of frequency for different angles of propagation at $\beta_T = 2$ and Mach 2.5.

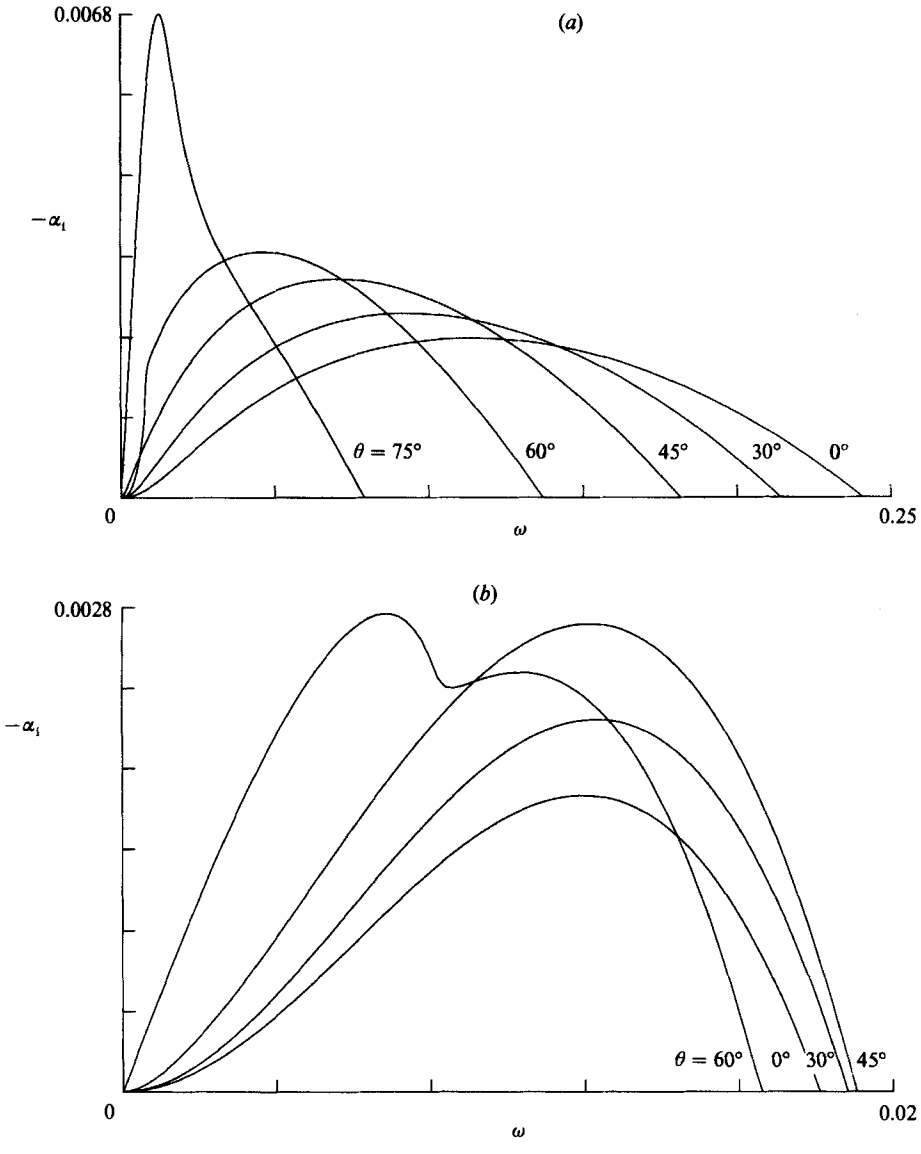

FIGURE 24. Plot of growth rates α_i for three-dimensional modes versus frequency for $\beta_T = 2$, $M = 5$: (*a*) fast modes; (*b*) slow modes.

Note the difference in the range of frequencies between the fast and slow modes. The maximum growth rate of the fast modes increases as θ increases up to about 60° and then decreases for larger angles of propagation. The range of unstable frequencies decreases as θ increases. The results given in figure 23(*b*) show that the slow modes have a different behaviour. The maximum growth rate occurs for two-dimensional waves and decreases as the angle increases and essentially disappears for $\theta > 20°$, because then the mode becomes subsonic.

Figure 24 shows the variation of the growth rate with frequency for both fast and slow modes for various angles of propagation at $\beta_T = 2$ and Mach 5. The results are similar to those of figure 23, but note the difference in magnitude. As the angle of

propagation increases the fast modes experience a decrease in the range of unstable frequencies and an increase in the growth rate; the maximum occurs at about $\theta = 75°$. The slow modes do not show much of an increase in maximum growth rate with angle of propagation. In contrast to Mach 2.5 case, the most unstable slow modes are three-dimensional.

We find, in agreement with Gropengiesser, that for low and moderate Mach numbers, the flow becomes less unstable as the stationary gas becomes hotter. He also stated that the growth rates decrease with increasing Mach number over the range of Mach numbers which he studied. This is certainly true for $M < M_*$, where one can see that there is a very rapid decrease in the maximum growth rate with increase in Mach number. For Mach numbers greater than M_*, we find that the rate of decrease is much smaller and eventually, at some moderate value of M, the growth rate begins to increase. Gropengiesser also found a second unstable mode for two-dimensional waves in a narrow range of Mach numbers, $1.54 < M < 1.73$. He stated that this second mode had a growth rate comparable with the first when $\theta = 30°$ and $\beta_T = 0.6$. Finally, he indicated that the growth rate of the second mode decreased sharply as β_T was increased. It is clear from the results presented in figures 6, 7, 8, and 14 that there will always be two groups of unstable modes if $M \geqslant M_*$. Of course these groups have different ranges of frequencies and will have quite different phase speeds.

4. Summary and conclusions

In this work we have considered the inviscid spatial stability problem for the compressible mixing layer with the mean velocity profile approximated by the hyperbolic tangent. We have found that there is only a single subsonic neutral mode for two-dimensional waves, but that there can be three for three-dimensional waves. Beyond the sonic curves the subsonic neutral modes are transformed into supersonic neutral modes which are subsonic at one boundary and supersonic at the other. We have not found any neutral or unstable modes whch are supersonic at both boundaries.

There are always at least two bands of unstable frequencies for Mach numbers greater than M_*. One of these bands is a group of fast and the other a group of slow unstable supersonic modes. The fast modes are supersonic with respect to the stationary stream and the slow modes are supersonic with respect to the moving stream. It is important to note that both the fast and slow supersonic modes are vorticity modes and neither of them is an acoustic mode (Mack 1989). These groups of unstable modes lie in the frequency bands between zero, corresponding to the sonic mode, and the frequency of the supersonic neutral mode. Because these frequency bands always overlap for some range of frequencies, there exist two unstable modes at a fixed Mach number and β_T for every frequency in this range. The phase speeds of both the fast and slow supersonic modes have a small range about the average, so that little dispersion of wave packets is expected, with a reduction in the dispersion as the Mach number is increased.

Three-dimensional disturbances show the same general characteristics as two-dimensional disturbances. There is always a range of propagation angles for which both the fast and slow unstable modes exist. We also find, in agreement with previous studies, that the maximum growth rate for any β_T and M occurs for three-dimensional waves.

A decrease in β_T results in an increase in the growth rate of the unstable waves at

any Mach number. An increase in the Mach number at a fixed β_T results in a decrease of the growth rates by a factor of 5 to 10 up to M_*. For Mach numbers greater than M_*, the growth rates level off and those of the slow modes begin to increase with increasing Mach number while those of the fast modes approach a limiting value. However, even at Mach 10, the growth rates are still small compared with those at low subsonic speeds. This, combined with the fact that the unstable waves have little dispersion, is a possible mechanism responsible for the observed increase in the flow stability.

We wish to acknowledge helpful conversations and comments from S. Cowley, J. P. Drummond, M. G. Macaraeg, L. M. Mack and M. V. Morkovin. This work was supported by the National Aeronautics and Space Administration under NASA Contract NAS1-18107 while the authors were in residence at the Institute for Computer Applications in Science and Engineering, NASA Langley Research Center, Hampton, VA 23665, USA.

REFERENCES

BLUMEN, W., DRAZIN, P. G. & BILLINGS, D. F. 1975 Shear layer instability of an inviscid compressible fluid. Part 2. *J. Fluid Mech.* **71**, 305–316.

BROWN, G. L. & ROSHKO, A. 1974 On density effects and large structure in turbulent mixing layers. *J. Fluid Mech.* **64**, 775–816.

CHAPMAN, D. R. 1950 Laminar mixing of a compressible fluid. *NACA Rep.* 958.

CHINZEI, N., MASUYA, G., KOMURO, T., MURAKAMI, A. & KUDOU, D. 1986 Spreading of two-stream supersonic turbulent mixing layers. *Phys. Fluids* **29**, 1345–1347.

DRAZIN, P. G. & DAVEY, A. 1977 Shear layer instability of an inviscid compressible fluid. Part 3. *J. Fluid Mech.* **82**, 255–260.

DUNN, D. W. & LIN, C. C. 1955 On the stability of the laminar boundary in a compressible fluid. *J. Aero. Sci.* **22**, 455–477.

GILL, A. E. 1965 Instabilities of 'top-hat' jets and wakes in compressible fluids. *Phys. Fluids* **8**, 1428–1430.

GROPENGIESSER, H. 1969 On the stability of free shear layers in compressible flows (in German). *Deutsche Luft. und Raumfahrt*, FB 69-25, 123 pp. also, *NASA Tech. Transl.* NASA TT F-12,786.

HO, C. M. & HUERRE, P. 1984 Perturbed free shear layers. *Ann. Rev. Fluid Mech.* **16**, 365–424.

JACKSON, T. L. & HUSSAINI, M. Y. 1988 An asymptotic analysis of supersonic reacting mixing layers. *Combust. Sci. Tech.* **57**, 129–140.

KUMAR, A., BUSHNELL, D. M. & HUSSAINI, M. Y. 1987 A mixing augmentation technique for hypervelocity scramjets. *AIAA Paper* 87-1882.

LEES, L. & LIN, C. C. 1946 Investigation of the stability of the laminar boundary layer in a compressible fluid. *NACA TN* 1115.

LESSEN, M., FOX, J. A. & ZIEN, H. M. 1965 On the inviscid stability of the laminar mixing of two parallel streams of a compressible fluid. *J. Fluid Mech.* **23**, 355–367.

LESSEN, M., FOX, J. A. & ZIEN, H. M. 1966 Stability of the laminar mixing of two parallel streams with respect to supersonic disturbances. *J. Fluid Mech.* **25**, 737–742.

LOCK, R. C, 1951 The velocity distribution in the laminar boundary layer between parallel streams. *Q. J. Mech. Appl. Maths* **4**, 42–63.

MACARAEG, M. G., STREETT, C. L. & HUSSAINI, M. Y. 1988 A spectral collocation solution to the compressible stability eigenvalue problem. *NASA Tech. Paper* 2858.

MACK, L. M. 1975 Linear stability theory and the problem of supersonic boundary-layer transition. *AIAA J.* **13**, 278–289.

MACK, L. M. 1984 Boundary layer linear stability theory. In *Special Course on Stability and Transition of Laminar Flow, AGARD Rep.* R-709, pp. 3-1–3-81.

MACK, L. M. 1987 Review of linear compressible stability theory. In *Stability of Time Dependent and Spatially Varying Flows* (ed. D. L. Dwoyer & M. Y. Hussaini), pp. 164–187. Springer.

MACK, L. M. 1989 On the inviscid acoustic-mode instability of supersonic shear flows. *Fourth Symp. on Numerical and Physical Aspects of Aerodynamic Flows, California State University, Long Beach, California.*

MICHALKE, A. 1972 The instability of free shear layers. *Prog. Aerospace Sci.* **12**, 213–239.

MONKEWITZ, P. A. & HUERRE, P. 1982 Influence of the velocity ratio on the spatial instability of mixing layers. *Phys. Fluids* **25**, 1137–1143.

PAPAMOSCHOU, D. & ROSHKO, A. 1986 Observations of supersonic free-shear layers. *AIAA Paper* 86-0162.

PAPAMOSCHOU, D. & ROSHKO, A. 1988 The compressible turbulent shear layer: an experimental study. *J. Fluid Mech.* **197**, 453–477.

RAGAB, S. A. 1988 Instabilities in the wake mixing-layer region of a splitter plate separating two supersonic streams. *AIAA Paper* 88-3677.

RAGAB, S. A. & WU, J. L. 1988 Instabilities in the free shear layer formed by two supersonic streams. *AIAA Paper* 88-0038.

STEWARTSON, K. 1964 *The Theory of Laminar Boundary Layers in Compressible Fluids.* Oxford University Press.

TAM, C. K. W. & HU, F. Q. 1988 Instabilities of supersonic mixing layers inside a rectangular channel. *AIAA Paper* 88-3675.

ZHUANG, M., KUBOTA, T. & DIMOTAKIS, P. E. 1988 On the instability of inviscid, compressible free shear layers. *AIAA Paper* 88-3538.